International Journal of Heat and Technology
Vol. 44, No. 2, April, 2026, pp. 529-536
Journal homepage: http://iieta.org/journals/ijht

Instructions for Preparing Heat Transfer Characteristics of Phase Change Material Based Heat Sinks Equipped with Curved Fins

Ahmad K. Al-Migdady*, Rami Al-Jarrah, Ahmad Al-Magableh

Department of Mechanical Engineering, Faculty of Engineering, the Hashemite University, Zarqa 13133, Jordan

Corresponding Author Email: a.k.almigdady@hu.edu.jo

https://doi.org/10.18280/ijht.440208

Received: 5 February 2026
Revised: 10 April 2026
Accepted: 17 April 2026
Available online: 30 April 2026

Keywords:
phase change material, finned heat sink, curved fins, heat transfer improvement

ABSTRACT

A rectangular heat sink filled with phase change material (PCM) (n-Eicosane) and subjected to a constant temperature on the left vertical side is numerically analyzed using ANSYS-FLUENT software without and with internal curved fins. The no-fin case reported a melting time of 213 minutes. Then, a single convex fin case and a single concave fin case were investigated, and the melting time was reduced to 83 and 75 minutes (61% and 65% reduction in melting time) for the convex and concave fin cases, respectively. After that, two fins were added to the heat sink and three configurations were studied: two convex fins, two concave fins, and mixed convex-concave fins. The melting time was reduced to 63 minutes (70% reduction in melting time) in the two convex fins, and in the last two cases, the melting time was reduced to 58 minutes (73% reduction in melting time).

1. INTRODUCTION

Electronic devices' performance, durability, and life span are greatly reduced by high temperatures; in fact, more than half of the electronics failures are due to high temperature [1]. Heat sinks are widely used to regulate their temperatures. Air-cooled heat sinks are more common but less effective in absorbing large amounts of heat loads. Phase change material (PCM) based heat sinks were introduced to absorb high amounts of the waste heat produced by electronic packages due to their high latent heat of fusion in a nearly isothermal process. The solid PCM melts as it absorbs the waste heat during peak operating periods and rejects this heat into the atmosphere at a later time, causing the PCM to solidify [2, 3].

However, the low thermal conductivity of PCMs around (0.2–0.4) $W/m^2 \cdot K$ [4] is considered a major limiting parameter to their performance; since low thermal conductivity slows the heat transfer process, and a high temperature gradient is present between the solid and liquid phases within the enclosure containing the PCM. This limitation is usually overcome by employing high thermal conductivity additives to PCM, like nano-particles, metal foams, and using extended surfaces and fins [5-8].

There are wide varieties of PCMs with a wide range of physical properties like: melting range, density, thermal conductivity, volume expansion, specific heats, and latent heat of fusion. PCM selection is typically related to the temperature control requirement for a certain application [9-11].

Basem et al. [12] used ANSYS-FLUENT software to investigate the heat transfer enhancement within a rectangular PCM based heat sink equipped with straight fins and V-shaped fins. The study demonstrated that fins actually accelerated the heat transfer process and the melting times were reduced by 50%.

Besides heat sinks application PCMs are also used in latent heat energy storage systems, Jadhav et al. [13] performed a numerical simulation of a PCM based latent heat storage system with numerous fin shapes, including triangular, rectangular, and leaf-shaped configurations, they reported melting time reduction by 26%, 47% and 64% for the triangular, rectangular, and leaf-shaped configurations, respectively when compared the plain tube case.

Çiçek [14] numerically investigated electronic cooling using PCM based finned heat sinks with different PCMs: RT-28HC, RT-31, and RT-54HC. The constant heat flux boundary condition was applied in all cases, and the lowest base temperature was achieved using RT-54HC due to its high latent heat and high melting temperature.

Zhang et al. [15] carried out a computational analysis of pin finned PCM based heat sink were carried out under the application of periodic heat flux pulses, they investigated the position and thickness of PCM and they recommended placing the heat sink in the middle of the channel for optimizing heat transfer and melting process, they also emphasized on selecting suitable PCM thickness to balance heat transfer rate with fluid resistance.

Bahrami and Saberi [16] carried out a CFD analysis to study the fin configuration effect on an annular PCM based thermal energy storage. They showed that melting time is reduced using larger fins, but such fins will limit PCM storage.

Msalmi et al. [17] conducted a computational study on a PCM based heat sink with various fin configurations: circular, triangular, and hexagonal, with different PCMs: RT44, n-Eicosane, and Paraffin wax. Constant heat flux was applied to the heat sink. They found out that n-Eicosane resulted in the best heat transfer enhancement, and triangular fins caused the most effective cooling.

Khalaf et al. [18] performed a CFD simulation using

ANSYS-Fluent to study the effects of the number and length of straight pin fins on the heat transfer dynamics in a hemispherical enclosure containing PCM. They reported a significant reduction in melting time with an increase in length and number of fins.

Yazdanparast et al. [19] carried out a numerical study on the performance of a PCM based regular finned enclosure under the application of a transient heat flux. The enclosure contained a blend of two types of PCM: lauric acid and paraffin wax, and the study examined the effect of the fin inclination angle, the number of fins, fin length, and the enclosure thickness. Results affirmed that the melting process is accelerated by adding more fins, using longer fins, and also with the inclination angle, whereas increasing the enclosure thickness resulted in an increase in the melting time.

In this work, a computational analysis is carried out using ANSYS-FLUENT software to investigate the heat transfer characteristics using a novel curved fin configuration in a rectangular enclosure containing PCM. The curved fins induce flow redirection and enhance mixing, and this yields a better convective heat transfer coefficient. They also maximize the area per unit length ratio, and a more uniform heat distribution is obtained.

The effect of the number of fins, as well as the convexity direction (convex and concave), is considered the main parameter of this study.

2. SIMULATION PROCEDURE

2.1 Physical models

A rectangular enclosure of 90 × 30 mm that is filled with PCM was considered in this study. A total 6 cases were investigated: in case (A) the heat sink contains no fins, in case (B) a single convex fin was employed, in case (C) two convex fins were employed, in case (D) single concave fin was employed, in case (E), two concave fins were employed and finally, in case (F), two fins with mixed orientation were employed: one convex and one concave. In all cases, each fin was a quarter circle with an inner radius of 20 mm and 1 mm thickness. Figure 1 shows the various geometries considered in this study. The heat sink was filled with n-Eicosane, which has the physical properties listed in Table 1.

Table 1. Thermo-physical properties of n-Eicosane

Property	Unit	Value
Density, ρ	kg/m^3	770
Heat capacity, c_p	J/kg-K	2460
Latent heat, L_f	kJ/kg	247.60
Thermal conductivity	W/m-K	0.1505
Dynamic viscosity	Pa s	0.00385
Solidus temperature, T_s	°C	35
Liquidus temperature, T_l	°C	37
Volume expansion coefficient, β	K^{-1}	0.0009

2.2 Mathematical modeling

The simulation of PCM melting process is well governed by the continuity, momentum, and energy equations [5-7] with the following assumptions being considered: Homogeneous and isotropic PCM with constant properties except for the density; Laminar, Newtonian, and incompressible flow; Boussinesq approximation was applied to account for the buoyancy effects; and finally, radiation effects as well as viscous dissipations were negligible.

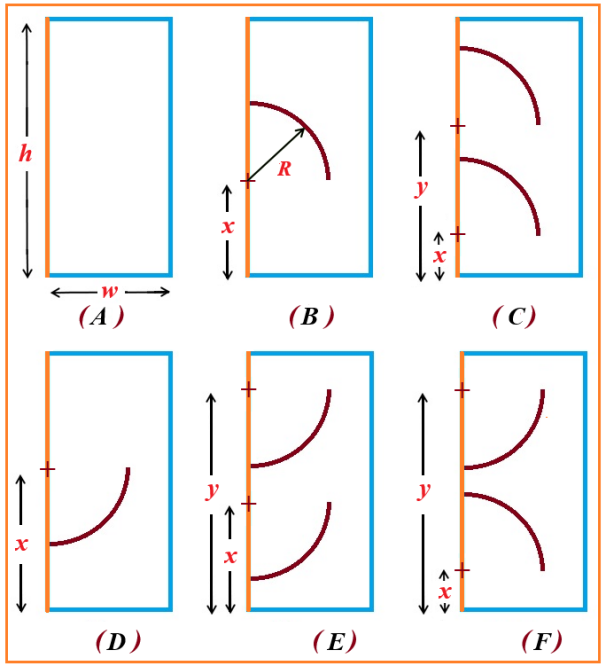

Figure 1. Heat sink geometry: case (a) h = 90 mm, w = 30 mm, case (b) x = 35 mm, case (c) x = 20 mm, y = 55 mm, case (d) x = 55 mm, case (e) x = 35 mm, y = 75 mm, case (f) x = 15 mm, y = 75 mm

The continuity equation can be written as:

$$\frac{\partial \rho}{\partial t} + \nabla . \rho \vec{u} = 0 \tag{1}$$

The momentum equation:

$$\frac{\partial \rho \vec{u}}{\partial t} + \nabla . (\rho \vec{u} \vec{u}) = \mu \nabla^2 \vec{u} - \nabla p + \rho \vec{g} \beta (T - T_{ref}) + \vec{S} \tag{2}$$

The energy equation will be:

$$\frac{\partial (\rho H)}{\partial t} + \nabla . (\rho \vec{u} H) = \nabla . (k \nabla T) \tag{3}$$

where, ρ: density, $\vec{u}$: velocity vector, p: pressure, μ: absolute viscosity, k: thermal conductivity, H: enthalpy, $\vec{S}$:source term; the momentum sink,

$$\vec{S} = \frac{(1-\alpha)}{\alpha^3 + \sigma} A_{mush} (\vec{u} - \vec{u}_p) \tag{4}$$

α: the liquid fraction, σ: a small scaler value to avoid division by zero, a preset value of 0.001 was chosen for σ, A_{mush} = the mushy zone constant, it is a measure of the damping amplitude, and it predicts the PCM behavior during melting/solidification. The value of the mush zone constant was set to 10^5, but it can vary between 10^4–10^7. $\vec{u}_p$: the pull velocity, which accounts for the solidified material movement away from the computational domain.

The total enthalpy H is the sum of the sensible enthalpy h and the latent heat ΔH:

$$H = h + \Delta H \tag{5}$$

$$h = h_{ref} + \int_{T_{ref}}^{T} c_p dT \tag{6}$$

using the latent heat of the material *(L_f)*, the latent heat content *(ΔH)* will be*:*

$$\Delta H = \alpha L_f \tag{7}$$

The latent heat content varies from 0 for the solid state to L_f for the liquid state.

The liquid fraction (α):

$$\alpha = \begin{cases} 0 & for\ T < T_s \\ \dfrac{T - T_s}{T_l - T_s} & T_s < T < T_l \\ 1 & for\ T > T_l \end{cases} \tag{8}$$

ANSYS FLUENT 20-R1 software was used to simulate and solve the mathematical model of the proposed heat sink; the melting process was detected by employing the enthalpy porosity approach, where the enthalpy balance is carried out at each iteration to compute both the melt fraction (α) and cell volume fraction in the liquid phase. Besides, the melt region of the PCM, which is represented by the mushy zone, is considered as a porous medium with liquid fraction varying from 0 for a total solid phase to 1.0 for a total liquid phase.

2.3 Initial and boundary conditions

Initially, the heat sink temperature was set to 34 ℃, which is below the melting point, and a full solidus state existed. A constant temperature of 52 ℃ was applied to the left side of the rectangular heat sink; all other sides were insulated. The added fins were attached to the heated left side of the enclosure, and they exhibited the same temperature.

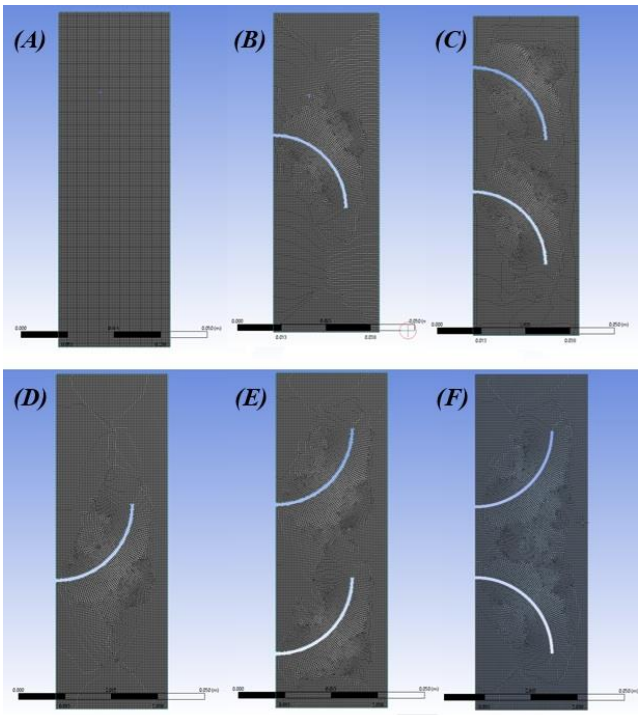

Figure 2. Meshing configurations of the various cases

2.4 Simulation details and validation

The design modeler was used to generate the heat sink geometry, and it was meshed using quadrilateral elements with almost 14600 elements in all cases. Figure 2 shows the meshed models of the six cases investigated.

The laminar flow was assumed due to low velocities. Also, the simple scheme for the pressure-velocity coupling was chosen, second-order wind spatial discretization was employed for both momentum and energy, whereas second-order implicit was used for the transient formulation.

The numerical procedure was validated against the work of Yang et al. [20], and Figure 3 shows a satisfactory agreement between the two results.

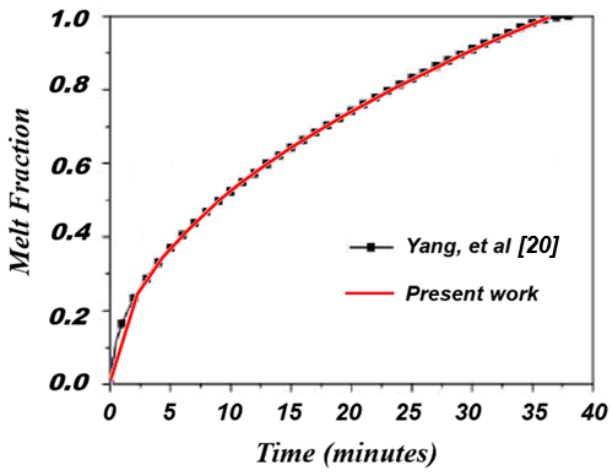

Figure 3. Melt fraction progress with time, validation against Yang et al. [20]

3. RESULTS AND DISCUSSIONS

3.1 No fin heat sink

Figure 4 shows the melting propagation of the No-fin case, Case (A), which took almost 213 minutes for the PCM to melt. At the start of the simulation, the heat sink is at 34 ℃ except for the heated left side, which is at 52 ℃. That is 15 ℃ above the PCM melting temperature. Heat transfer is initiated in the vicinity of the heated surface via conduction and gradually propagates through the PCM. In the early stages of melting, conduction dominates the heat transfer process. The melting region propagates with time, and temperature gradients cause buoyancy effects, and consequently, convection currents are formed and enhanced mixing is present in the molten region, and convection dominates the heat transfer process. The temperature of the molten PCM rises as it keeps receiving heat from the hot side, whereas the solid PCM is at its initial temperature. Eventually, all the PCM melts, and after that, only sensible heating is present.

The inclination of the solid-liquid interface from bottom left to top-right, which becomes more obvious at higher melt fractions, is caused by the clockwise natural convection currents, and hence, induced heat transfer enhancement is present in the upper region of the molten PCM, while the less effective conduction is present in the lower side of the heat sink, causing slower melting of the PCM. In fact, natural convection with the absence of any conductive heat transfer enhancements is insufficient to accelerate heat transfer or to cause uniform melting.

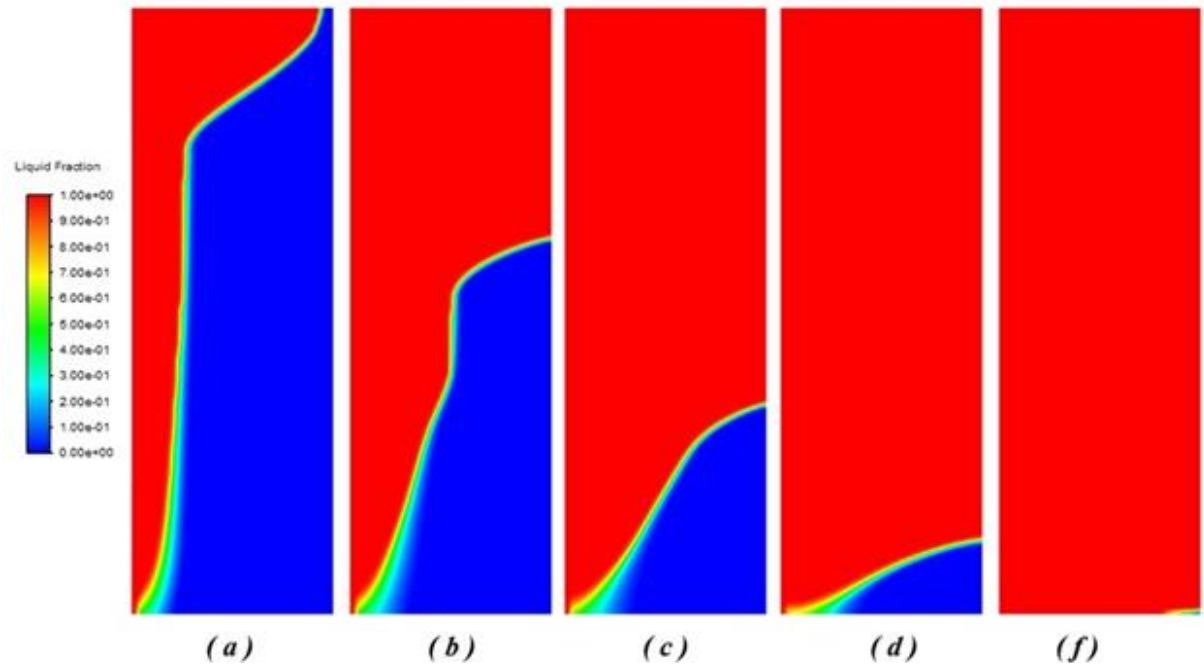

Figure 4. Contours of melt fractions, Case A at t = 40, 90, 140, 170, 213 minutes

3.2 Single curved fin heat sink

Figures 5 and 6 illustrate the melting propagation a heat sink integrated with one convex fin, case (B) and one concave fin, case (D), respectively, the melting time is reduced to 83 minutes in the convex fin case and 75 minutes in the concave fin case which corresponds to a 61% and 65%-time reduction for case B and case D, respectively, when compared to the no-fin case. The curved fin significantly improves the heat transfer from the heated edge to the interior of the heat sink. The fin breaks the molten region into two zones and improves convection currents speed the melting process. After 40 minutes, most of the PCM above and adjacent to the fin is molten, and the rest of the time was consumed to melt the PCM in the lower right corner, where slow conduction heat transfer takes place. Further time reduction can be obtained by lowering the position of the fin.

3.3 Two curved fin heat sink

Figures 7, 8, and 9 show the progress of the liquid fraction for a PCM based heat sink with two fins: case (C), case (E), and case (F), respectively. The heat transfer rate improvement is well demonstrated in all cases: the two-fin configuration accelerates the heat transfer and melting rate accordingly by breaking the molten PCM into three zones in which convection currents are dominant and enhanced mixing improves heat transfer significantly, causing more than 75% of the PCM to melt within the first 30 minutes. Once the PCM surrounding the fins is molten, sensible heating raises the molten PCM temperature, and the remaining solid PCM away from the fins keeps melting upon the action of slow rate conduction heat transfer, and this extends the melting process for about the next 30 minutes.

The PCM melting progress with time is plotted in Figure 10 for all cases, and the inset plot shows the liquid fraction progress for the finned cases. It's quite obvious that fin addition significantly reduces the melting time.

In the single fin cases, the slope of the liquid fraction curve for the concave fin case is greater than that of the convex fin case, especially in the early stages of melting, where strong convection currents dominate heat transfer, and then melting is reduced by the slow conduction heat transfer away from the heat conducting fins.

Similar behavior is observed in the two fin configuration cases: where in the early stages of melting, the melting rate in case (E) with two concave fins is higher than that of case (F) with two type fins, and case (C) with the two convex fins has the least melting rate. In fact, most of the PCM was molten in the first half of the simulation, and the rest of the time was consumed to melt the PCM away from the fins, where slow conduction dominates heat transfer.

The variations in the average Nusselt number with time in the PCM for various cases are shown in Figure 11. The Nusselt number is the highest in the two-fin case and lowest in the no-fin case. The curved fins induce flow redirection and improve mixing, and as a result, a better convective heat transfer coefficient is obtained.

Initially, the PCM is entirely solid, and heat transfer is dominated by conduction only. The temperature gradient is steep near the hot surface, a high initial Nusselt number is obtained (due to the large temperature gradient), and as the thermal boundary layer grows with time, the Nusselt number rapidly decreases. Upon PCM melting near the hot surface, a thin liquid layer is formed, and convection current starts to develop. In the early stages of melting, the liquid layer is very thin, and convection is negligible. Nusselt number continues to decrease, reaching a minimum value which corresponds to the transition from pure conduction to convection.

Further melting causes the liquid region to increase in size, and strong convection currents are formed, dominating heat transfer. In fact, heat transfer is significantly higher than that of pure conduction. As melting continues, the melt front propagates, and the solid PCM size is reduced, and temperature gradients get weaker, and as a result, the Nusselt number gradually decreases as the system is heading towards thermal equilibrium.

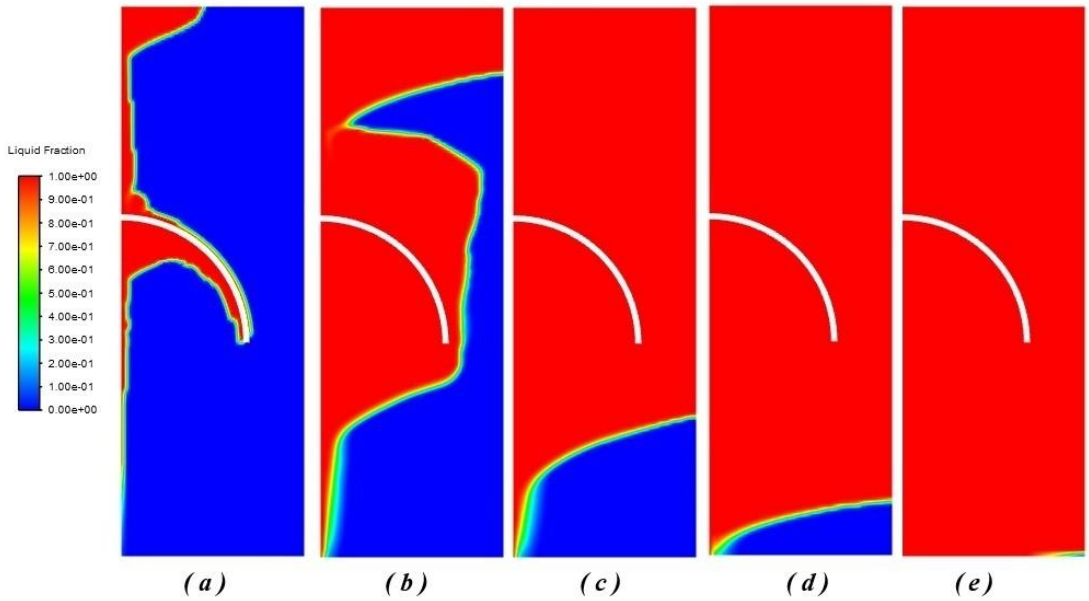

Figure 5. Contours of melt fractions, Case B at t = 10, 20, 40, 60, 80 minutes

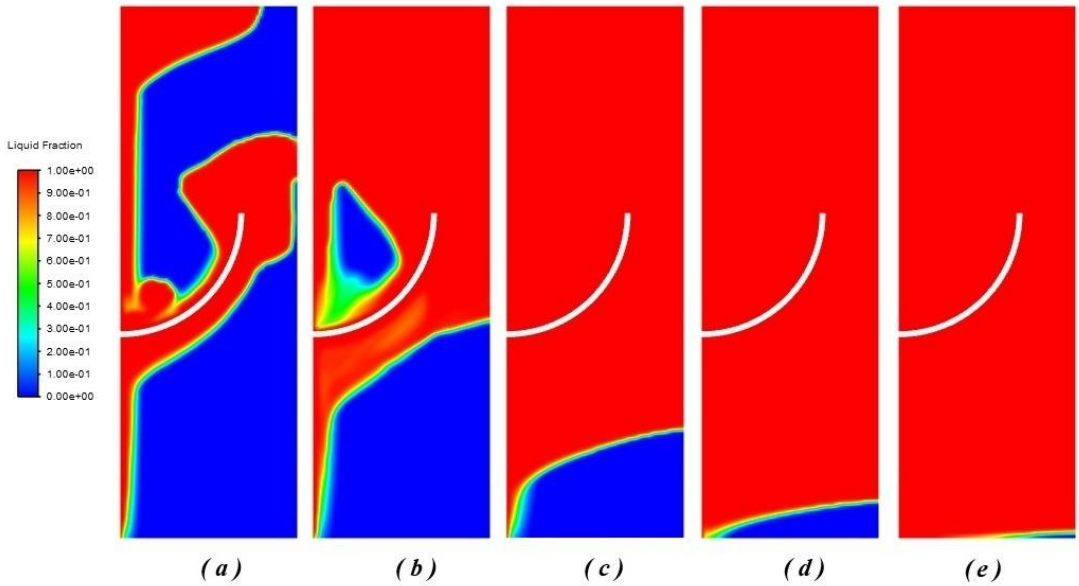

Figure 6. Contours of melt fractions, Case D at t = 10, 20, 40, 60 and 75 minutes

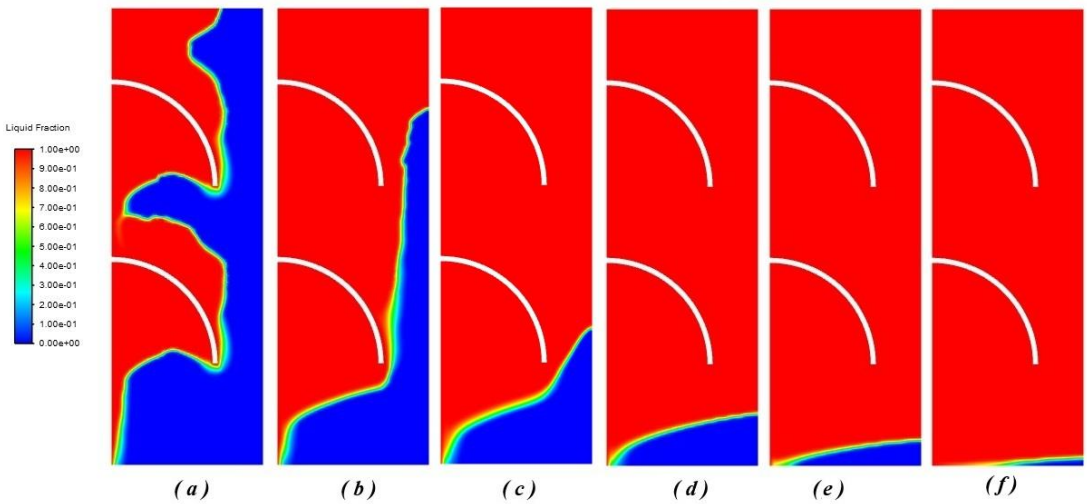

Figure 7. Contours of melt fractions, Case C at t = 10, 20, 30, 40, 50 and 60 minutes

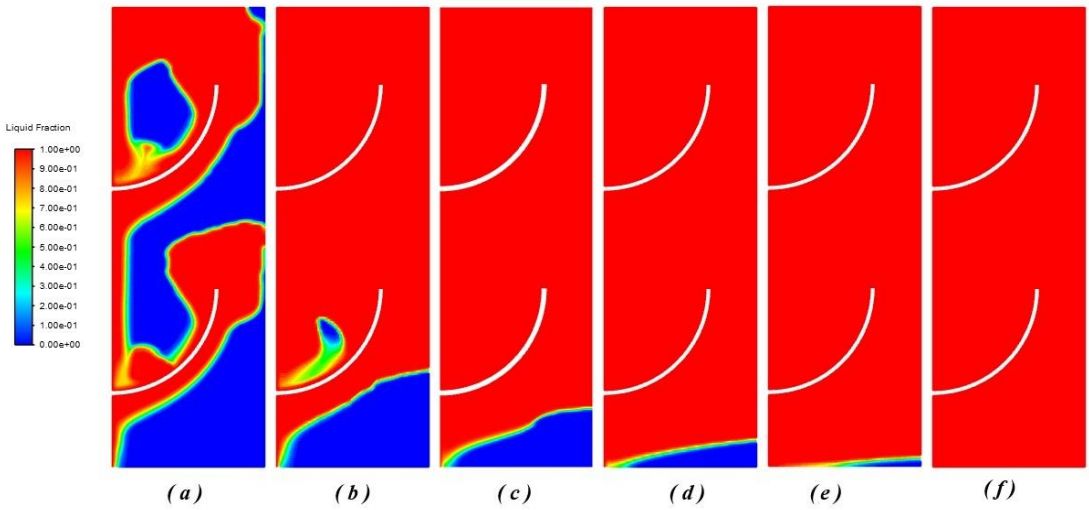

Figure 8. Contours of melt fractions, Case E at t = 10, 20, 30, 40, 50 and 60 minutes

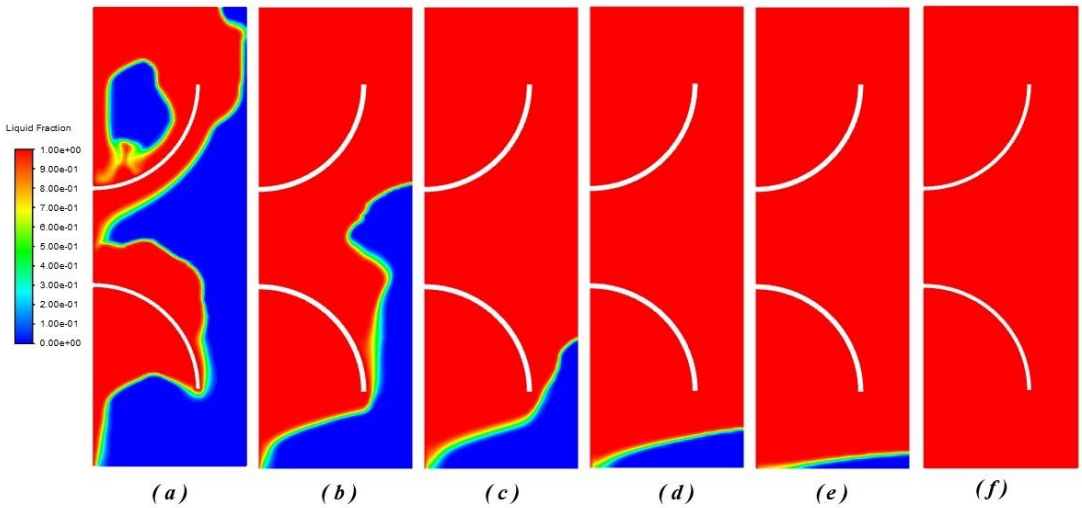

Figure 9. Contours of melt fractions, Case F at t = 10, 20, 30, 40, 50 and 60 minutes

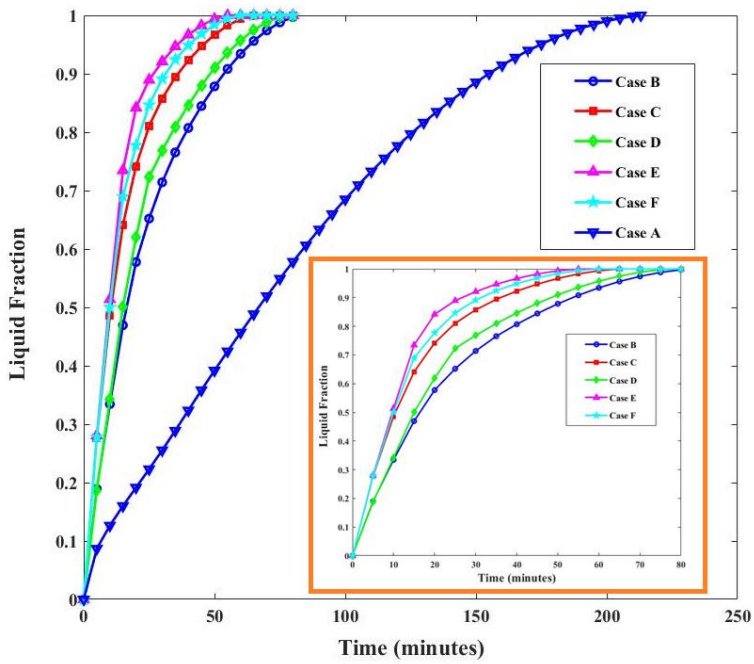

Figure 10. Melt fraction progress with time, all cases; inset: Cases B–F

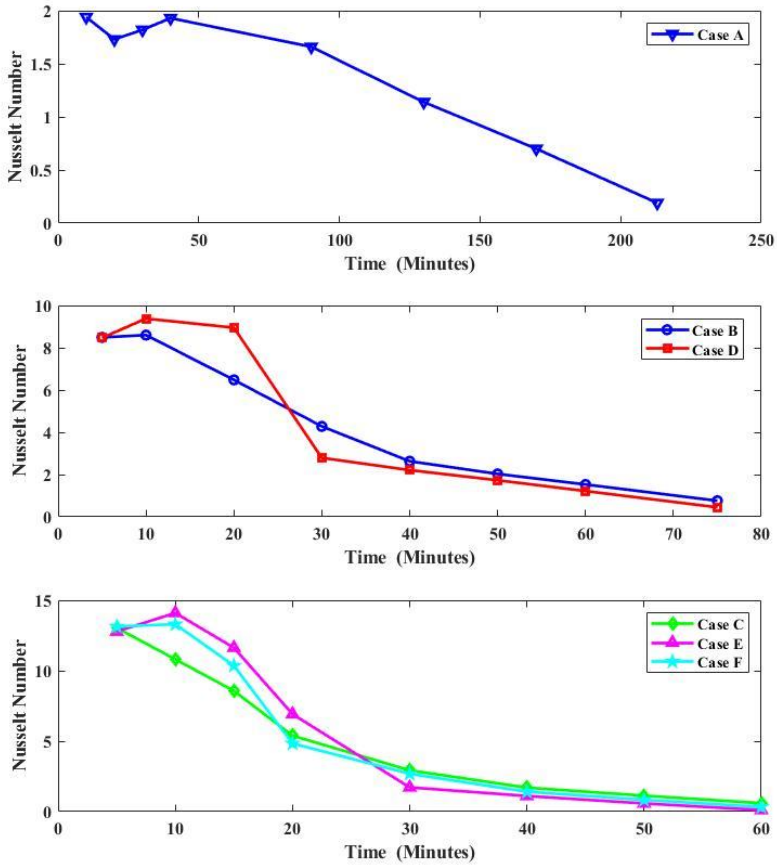

Figure 11. Variations of the average Nusselt number of the phase change material (PCM) with time

4. CONCLUSIONS

This study computationally investigated the heat transfer improvement in a rectangular PCM based heat sink with and without curved fins. The computational domain was successfully simulated using ANSYS-FLUENT software using the enthalpy-porosity approach; furthermore, a constant temperature heated vertical side boundary condition was employed.

The added fins affected the heat transfer process, increased convection currents, and accelerated the melting rate, and eventually, a substantial reduction in melting time was recorded.

The results showed a 61% and 65% reduction in melting time in the single convex fin case and the single concave fin case, respectively, when compared to the no fin case.

Adding more fins caused further heat transfer enhancement and further reduction in melting time. The simulation results showed a 70% reduction in melting time for the two convex fin case, and about 73% reduction in melting time for the two concave fin case and two mixed fin configuration case as well.

Heat transfer characteristics in the concave fin cases were slightly better than those in the convex cases.

Fin placement is very important for heat transfer enhancement, as well as the number of fins and convexity.

Although curved fins can be utilized for passive cooling and in Latent heat energy storage devices, manufacturing complexity can limit their usage. Sometimes, with poor design and placement, they can trap liquid PCM in dead zones. PCM circulation paths may be restricted and reduce effective heat transfer locally, and overlap between fins as well as between fins and enclosure needs to be avoided.

Further better heat transfer performance and melting time reduction can be achieved by optimizing the fin placement, also altering the geometry of the lower left corner of the heat sink by replacing the 90° corner with a chamfer or a round fillet that has a comparable curvature to the fin.

Besides, considering heat sinks with a horizontal hot surface will cause a more uniform heat transfer and less melting time.

A different set of analyses can be carried out for constant heat flux boundary conditions.

REFERENCES

[1] Alawadhi, E., Amon, C. (2000). Performance analysis of an enhanced PCM thermal control unit. In ITHERM 2000. The Seventh Intersociety Conference on Thermal and Thermomechanical Phenomena in Electronic Systems, Las Vegas, NV, USA. https://doi.org/10.1109/ITHERM.2000.866837

[2] Py, X., Olives, R., Mauran, S. (2001). Paraffin/porous-graphite-matrix composite as a high and constant power thermal storage material. International Journal of Heat and Mass Transfer, 44(14): 2727-2737. https://doi.org/10.1016/s0017-9310(00)00309-4

[3] Clarksean, R., Chen, Y. (1999). The use of phase change material for electronic cooling application: Thermal design issues and example. In Proceedings of the Pacific Rim/ASME International Intersociety Electronic and Photonic Packaging Conference (InterPACK '99), pp. 1631-1640.
[4] Tian, Y., Zhao, C. (2011). A numerical investigation of heat transfer in phase change materials (PCMs) embedded in porous metals. Energy, 36(9): 5539-5546. https://doi.org/10.1016/j.energy.2011.07.019
[5] Al-Migdady, A.K., Jawarneh, A.M., Dalgamoni, H.N., Tarawneh, M. (2020). Combined effects of eccentricity and internal fins on the shell and tube latent heat storage systems. International Journal of Recent Technology and Engineering (IJRTE), 9(1): 230-236. https://doi.org/10.35940/ijrte.f9537.059120
[6] AL-Migdady, A.K., Jawarneh, A.M., Ababneh, A.K., Dalgamoni, H.N. (2021). Numerical investigation of the cooling performance of PCM-based heat sinks integrated with metal foam insertion. Jordan Journal of Mechanical & Industrial Engineering, 5(2): 191-197.
[7] Al-Migdady, A.K. (2021). Temperature regulation of photovoltaic cells using phase change material heat sinks integrated with metal foam. Journal of Physics: Conference Series, 1888(1): 012001. https://doi.org/10.1088/1742-6596/1888/1/012001
[8] Jawarneh, A.M., AL-Migdady, A.K., Ababneh, A.K., Tlilan, H.M., Tarwaneh, M. (2023). Measurement and assessment of solar energy in Zarqa Governorate-Jordan. Jordan Journal of Mechanical & Industrial Engineering, 17(4): 605-615. https://doi.org/10.59038/jjmie/170415
[9] Das, D., Crosby, R., Paul, M.C. (2025). A comprehensive review on the form stable phase change materials for storing renewable heat preparation, characterization and application. Journal of Energy Storage, 110: 115284. https://doi.org/10.1016/j.est.2024.115284
[10] Calborean, A., Máthé, L., Bruj, O. (2025). Phase change materials for thermal management in lithium-ion battery packs: A review. Batteries, 11(12): 432. https://doi.org/10.3390/batteries11120432
[11] Yao, Y., Li, W., Liu, J., Deng, Z. (2024). Liquid metal phase change materials for thermal management of electronics. Advances in Physics: X, 9(1): 2324910. https://doi.org/10.1080/23746149.2024.2324910
[12] Basem, A., Al-Tajer, A.M., Omar, I., Dhahad, H.A., Alawee, W.H. (2024). Improvement of heat transfer within phase change materials using V-shaped rods. Heliyon, 10(7): e28146. https://doi.org/10.1016/j.heliyon.2024.e28146
[13] Jadhav, R., Sable, M.J., Bhalla, V., Jadhav, P.K., Sawant, H.H., Konkala, B., Marlapalle, B.G., Gawande, S.H. (2025). Optimization of fin arrangements in latent heat storage systems. Mathematical Modelling of Engineering Problems, 12(2): 601-608. https://doi.org/10.18280/mmep.120223
[14] Çiçek, B. (2024). Numerical investigation on thermal behaviors of heat sinks and hybrid heat sinks with different PCMs for electronic cooling. Advances in Mechanical Engineering, 16(8): 16878132241269229. https://doi.org/10.1177/16878132241269229
[15] Zhang, D., Yang, L., Kong, X., Lu, X. (2025). Thermal control performance of a novel PCM-based pin fin hybrid heat sink. Journal of Energy Storage, 131: 117630. https://doi.org/10.1016/j.est.2025.117630
[16] Bahrami, H., Saberi, M. (2024). Thermal optimization of PCM-based heat sink using fins: A combination of CFD, genetic algorithms, and neural networks. The Journal of Engineering, 2024(10): 70015. https://doi.org/10.1049/tje2.70015
[17] Msalmi, A., Djemal, F., El Hami, A., Haddar, M. (2024). Numerical investigation of finned heat sinks with PCM for electronics thermal management: A parametric study. In International Conference on Integrated Design and Production, Monastir, Tunisia, pp. 230-239. https://doi.org/10.1007/978-3-032-04742-7_23
[18] Khalaf, A.F., Rashid, F.L., Al-Obaidi, M.A., Mohammed, H.I., Ameen, A., Agyekum, E.B. (2025). Enhancing thermal performance of phase change materials using conductive rods with length dependent melting dynamics. Scientific Reports, 15(1): 1-16. https://doi.org/10.1038/s41598-025-17040-y
[19] Yazdanparast, S.A., Setareh, M., Tabrizi, H.B. (2026). Numerical investigation of melting characteristics of fin-assisted single and dual PCM latent heat storage system under time-dependent solar heat flux. Discover Mechanical Engineering, 5(1): 14. https://doi.org/10.1007/s44245-026-00185-z
[20] Yang, X., Tan, S., Liu, J. (2016). Numerical investigation of the phase change process of low melting point metal. International Journal of Heat and Mass Transfer, 100: 899-907. https://doi.org/10.1016/j.ijheatmasstransfer.2016.04.109

NOMENCLATURE

$Amush$	the mushy zone constant
C_p	specific heat, J/kg·K
H, h	enthalpy, kJ/kg
k	thermal conductivity, W/m^2·K
L_f	latent heat of fusion, kJ/kg
p	pressure, kPa
S	Darcy's Momentum sink, N/m^3
t	time, s
T	temperature, K
T_s	solidus temperature, K
T_l	liquidus temperature, K
u	velocity vector, m/s

Greek symbols

α	liquid fraction
β	thermal expansion coefficient, 1/K
ρ	density, kg/m^3
μ	dynamic viscosity, Pa·s